Differential roles of extracellular matrix proteins on primary and metastatic pancreatic cancer cells

Olalekan H Usman[1], Sampath Kumar[1], Reddick R Walker III[1], Gengqiang Xie[1], AbdelAziz R. Jalil[3], Subramanian Ramakrishnan[2], Lawrence J. Dooling[3], Yue Julia Wang[1], Jerome Irianto[1]*

[1]Department of Biomedical Sciences, College of Medicine, Florida State University, Tallahassee, FL, USA

[2]Department of Chemical and Biomedical Engineering, FAMU-FSU College of Engineering, Tallahassee, FL, USA

[3]Physical Sciences Oncology Center at Penn, University of Pennsylvania, Philadelphia, PA, USA

*Corresponding author: Jerome Irianto, Department of Biomedical Sciences, College of Medicine, Florida State University, 1115 West Call St, Tallahassee, FL 32306.

Phone: 850-645-9438

E-mail: jerome.irianto@med.fsu.edu

Abstract

Pancreatic cancer adenocarcinoma (PDAC) has been reported to be the third highest cause of cancer-related deaths in the United States. PDAC is known for its high proportion of stroma which accounts for 90% of the tumor mass. The stroma is made up of extracellular matrix (ECM) and non-malignant cells such as inflammatory cells, cancer-associated fibroblasts (CAF), and lymphatic and blood vessels. Here, we decoupled the roles of the ECM on PDAC cell lines by culturing the cells on surfaces coated with different ECM proteins. Our data showed that the primary tumor-derived cell lines have different morphology that depends on the ECM proteins on which they are cultured, while metastatic lesion-derived PDAC lines' morphology does not change with respect to the different ECM proteins. Similarly, ECM proteins also modulate the proliferation rate and the gemcitabine sensitivity of the primary tumor PDAC cell lines, but not for the metastatic PDAC lines. Lastly, transcriptomics analysis of the primary tumor PDAC cells cultured on different ECM proteins reveals the regulation of various pathways, such as cell cycle, cell adhesion molecules, and focal adhesion, including the regulation of several integrin genes that are essential for ECM recognition.

Introduction

Pancreatic cancer adenocarcinoma (PDAC) has been reported to be the third highest cause of cancer-related deaths in the United States and it is predicted to be ranked second before 2030, replacing colorectal cancer [1, 2]. Although, in general, there has been a downward trend in the number of cancer deaths with a 32 percent decrease from its peak in 1991 and 2019 [3], PDAC has been an exception, with less than 5% of the patients surviving for 5 years [4]. This poor prognosis has been attributed to the difficulty in early-stage diagnosis due to the lack of specific tumor markers, resistance to radiotherapy, chemotherapy, and molecular targeted therapy [5]. PDAC is known for its high proportion of stroma which accounts for 90% of the tumor mass [6]. The stroma is made up of extracellular matrix (ECM) and non-malignant cells such as inflammatory cells, cancer-associated fibroblasts (CAF), and lymphatic and blood vessels. These stromal components are in a bidirectional dynamic interaction with the tumor cells [7]. Tumor fibrotic stroma has been a major contributor to PDAC progression, and invasion, together with resistance to treatment [8,9]. The resulting stiffness from high stroma deposition in PDAC can also result in deformation of the vasculature, thereby limiting oxygen, nutrients, and drug transport to the tumor cells [10].

The extracellular matrix is a highly organized three-dimensional meshwork that surrounds and provides physical support for the cells [11]. ECM is mainly made up of glycoproteins and fibrous proteins that include collagens, fibronectin, laminin, vitronectin, proteoglycans, and elastin [12, 13]. The reorganization, density, posttranslational modifications, and remodeling of its constituent proteins confer the ECM the ability to respond to both biochemical and mechanical cues from the tumor microenvironment [14]. In this study, we decided to focus on collagen I, fibronectin, laminin, and vitronectin. Of the 28 collagens that have been identified, collagen I is known to promote tumorigenesis, and immunohistochemistry staining from different studies showed a significantly high level of the protein in both mouse and human PDAC samples [15, 16]. Collagen I, together with collagen III makes up approximately 80% of the ECM mass [17]. The crosslinking of collagen I and its remodeling by proteases have been implicated in tumor progression processes including invasion [18], and resistance to cell death [19]. In addition, Olivares and colleagues have shown that collagen can be a source of proline (one of its components) which can serve as fuel for the cancer cells when other nutrients are limited [15]. Fibronectin is a key glycoprotein in the extracellular matrix which has been reported to be required for the assembly and deposition of other ECM proteins including collagen I [20]. Fibronectin contributes to tumor progression and dormancy by increasing proliferation signaling via integrins clustering [21], inhibiting apoptosis [22], and promoting the

formation of a pre-metastatic niche [23]. In addition, in small-cell lung cancers, fibronectin has been reported to promote chemoresistance to drugs such as etoposide and doxorubicin [23, 24]. Laminin is involved in providing tensile strength in the basement membrane which helps to maintain the apical-basal polarity of epithelial structures [25]. Different groups have shown that laminin expression correlates with tumor invasion [26] [27]. In a similar manner to other ECM proteins mentioned above, vitronectin acts as an adhesive, connecting the cells to the matrix through integrins. A high level of vitronectin level in neuroblastoma correlates with poor prognosis [28].

Here, we decoupled the roles of the ECM on PDAC cell lines by culturing the cells on surfaces coated with different ECM proteins. Our data showed that primary tumor-derived cell lines have different morphology that depends on the ECM proteins on which they are cultured while metastatic lesion-derived PDAC lines' morphology does not change with respect to different ECM proteins. Next, we examined how these ECM proteins affect cell proliferation rate and cell sensitivity to gemcitabine's cytotoxicity. Similar to the cellular morphological findings, ECM proteins only modulate the proliferation rate and the gemcitabine sensitivity of the primary tumor PDAC cells. Lastly, transcriptomics analysis showed differential expression of genes involved in pathways such as cell cycle, DNA replication, focal adhesion, MAPK signaling pathway, and more, when the primary tumor PDAC cells were cultured on different ECM proteins. Finally, we observed differential regulations of multiple integrins for cells cultured on vitronectin and fibronectin which might explain the uniquely regulated pathways in the two ECM proteins.

Results

Extracellular matrix proteins have different effects on PDAC cell lines morphology and proliferation

To study the effect of extracellular matrix proteins on the morphology of the cell, primary tumor PDAC cell lines (MIA PaCa-2 and PANC-1) were seeded at approximately 3200 cells/cm^2 and cultured for 6 days in well plates coated with laminin, collagen I, fibronectin and vitronectin using culture media supplemented with 2% B27. In this ECM study, the culture media was supplemented with the serum-free supplement, B27, instead of the conventional fetal bovine serum (FBS). This is mainly because FBS consists of albumin, growth factors, and other proteins including the ECM proteins, like fibronectin, that can be deposited on the culture surface and interact with the cells during the culture, which may confound our observations [29]. Microscopy imaging shows that MIA PaCa-2 spreads in wells coated with fibronectin and vitronectin, similar to cells grown in 10% FBS media. Meanwhile, the MIA PaCa-2 cells are rounded in laminin and

collagen in a manner similar to cells grown on a plate with no ECM protein coating (**Figure 1Ai top**). The PANC-1 line adheres and spreads on fibronectin, vitronectin, and collagen I substrates while they were rounded on laminin **(Figure 1Ai bottom)**. We quantified the morphology of the cells grown on each ECM protein by measuring the aspect ratio of the cells. Our quantification agrees with the observation above, where the aspect ratio is higher for MIA PaCa-2 cells cultured on fibronectin and vitronectin **(Figure 1Aii)**, and for PANC-1 cells cultured on collagen I, fibronectin, and vitronectin **(Figure 1Aiii)**. AsPC-1 and Capan-1, which are derived from metastatic sites of PDAC patients [30], were also cultured on plates coated with different ECM proteins. Microscopy imaging reveals that these cell lines moderately spread on all ECM coatings and wells with no ECM coating **(Figure 1Bi)**. The aspect ratio quantification showed that the morphology of the cell lines does not change with respect to the different ECM proteins **(Figure 1Bii-iii)**. Capan-1 cells are often clustered together, and to quantify their aspect ratio, we stained the cells' nuclei and filamentous actin (F-actin), allowing us to differentiate individual cells within the clusters **(Figure S1)**.

Next, we studied the effect of ECM proteins on the growth of the cell lines using a luminescence assay. The number of cells under each condition was quantified on days 2, 4, and 6 using a luminescent cell viability assay and normalized to the number of cells seeded. Resonating with the morphology findings, MIA PaCa-2 on fibronectin and vitronectin-coated surfaces have a significantly higher proliferation rate when compared to those cells on laminin and collagen I **(Figure 1Ci)**, suggesting the correlation between cell spreading and proliferation rate. The same for the spreading PANC-1 cells cultured on fibronectin, collagen I, and vitronectin, they double faster relative to those cultured on laminin **(Figure 1Cii)**. For AsPC-1 and Capan-1 cells, their proliferation rates were not significantly influenced by any of the ECM proteins **(Figure 1Ciii-iv)**.

Extracellular matrix proteins alter cell response to gemcitabine

Gemcitabine is an analog of deoxycytidine that inhibits the elongation step during DNA synthesis and consequently, prevents cell growth. [31,32]. It is used as the first-line treatment for PDAC patients [33]. However, after a few weeks of treatment, most patients become resistant to the drug [34]. To assess the cytotoxic effect of gemcitabine on the cell lines **(Figure 2A)**, we treated them with gemcitabine for 72 hours and the cell numbers were quantified using a luminescence cell viability assay. We found that MIA PaCa-2 and Capan-1 are more sensitive to the drug treatment, with half maximal inhibitory concentration (IC50) of 10.8 and 2.8 nM, compared to PANC-1 and AsPC-1 with IC50 of 544.2 and 652.9 nM, respectively **(Figure 2B).**

PDAC is known for its high stroma which has been implicated in chemoresistance [35]. Next, we tested the effect of ECM proteins on the cytotoxic effect of gemcitabine on MIA PaCa-2 and Capan-1. Towards this, we cultured MIA PaCa-2 on surfaces coated with different ECM proteins, followed by the gemcitabine treatment and the luminescence cell viability assay. The cell viability plot shows that the total number of surviving cells after gemcitabine treatment is the lowest for cells cultured in FBS, followed by the cells cultured on fibronectin and vitronectin (ECM proteins in which the cell has a spread morphology) compared to no ECM, **(Figure 2C)**, suggesting the correlation between cell spreading and gemcitabine sensitivity. In contrast, ECM proteins do not significantly alter the decrease in the number of surviving cells following drug treatment in Capan-1 cells **(Figure 2D)**.

ECM proteins result in differential gene expression

To investigate the roles of different ECM proteins on MIA PaCa-2 gene expression, RNA-seq analyses were performed on MIA PaCa-2 cells that were cultured on different ECM-coated surfaces for 6 days. MIA PaCa-2 cell line was chosen for this experiment because it is one of the lines that showed differences in morphology, growth, and gemcitabine sensitivity with respect to different ECM proteins. The gene count across the conditions was normalized using the variance stabilizing transformation from DESeq2 [36]. The sample clustering was visualized by plotting the first two components resulting from PCA analysis on the x and y axes respectively **(Figure 3A)**. PCA analysis showed that cells cultured on ECM proteins (collagen I, laminin) that result in rounded morphology clustered together with cells grown on no ECM. Interestingly, cells cultured on ECM proteins that result in spread morphology (fibronectin and vitronectin) cluster separately from each other, and the cells cultured in FBS. These results suggest that the ECM proteins on which the cells were cultured can modulate gene expression of the cells. Next, to show the differences in the gene expression pattern of cells cultured on different ECMs, the differentially regulated genes were visualized in a heatmap **(Figure 3B)**. The sample hierarchical clustering analysis reveals that cells cultured on collagen I, laminin, and no ECM protein have a similar expression pattern while those cultured on fibronectin, vitronectin, and FBS show differential gene expression patterns, confirming our findings from the PCA analysis. The K-mean clustering of the genes reveals four distinct clusters of genes: cluster 1 comprises genes that are highly upregulated in cells cultured in FBS, while also generally upregulated in cells cultured on vitronectin and fibronectin. Cluster 2 comprises genes that are downregulated in cells cultured in FBS. Clusters 3 and 4 comprise genes that are upregulated and downregulated in cells cultured

on a surface coated with vitronectin, respectively. To investigate the regulated pathways, we performed functional annotation analysis on the genes within each cluster by using Enrichr [37]. Cluster 1 contains genes that are upregulated in FBS and are enriched for cell cycle, DNA replication, RNA transport, spliceosome, and other pathways **(Figure 3Ci)**. Cluster 2 consists of genes that are uniquely downregulated in FBS and are enriched in pathways involving lysosome and glycosaminoglycan **(Figure 3Cii)**. Cluster 3 is made up of genes that are uniquely upregulated in vitronectin and enriched in pathways that include MAPK signaling, cell adhesion molecules, the Wnt signaling pathway, and others **(Figure 3Ciii)**. Cluster 4 contains genes that are uniquely downregulated in vitronectin and are enriched in pathways such as terpenoid backbone biosynthesis, endocytosis, and focal adhesion **(Figure 3Civ)**.

One of the major receptors of ECM proteins is the integrins, which are heterodimeric proteins found in the plasma membrane that connect the cells with the ECM by binding to specific recognition sites on the ECM ligands [38, 39]. In addition to focal adhesion formation, integrins are also involved in cell migration [40], bidirectional biochemical, and mechanical signal transduction between the cell and the ECM [41]. MIA PaCa-2 cells express a range of integrin genes (**Figure S2**), which potentially enable the interactions with the RGD motif within fibronectin and vitronectin through α5β1, αVβ1, αVβ5, αVβ6, and αVβ8 integrins, the laminin proteins through α3β1, α6β1, α7β1, α10β1, and α6β4 integrins, and also the collagen I proteins through α10β1 integrin [38, 39].

Both the PCA analysis **(Figure 3A)** and the clustering analysis of the differentially expressed genes **(Figure 3B)** show that MIA PaCa-2 cells respond differently when cultured on fibronectin and vitronectin. This prompted us to take a closer look at the genes that are co-regulated and uniquely regulated between the two ECM proteins. For the upregulated genes, 167 genes were upregulated in both fibronectin and vitronectin cultured cells, while 868 and 126 genes were uniquely upregulated in vitronectin and fibronectin, respectively **(Figure 4Ai)**. For the downregulated genes, 335 genes were downregulated in both fibronectin and vitronectin, while 1265 and 297 genes were uniquely downregulated in vitronectin and fibronectin, respectively **(Figure 4Aii)**. Distinct signaling pathways were enriched by each of the gene lists above **(Figure S3)**. Interestingly, we observed differential expression of several integrin genes in MIA PaCa-2 cells cultured on vitronectin and fibronectin (**Figure 4B)**. Both *ITGB8* and *ITGA6* were downregulated in cells cultured on fibronectin and vitronectin. *ITGA10* was uniquely downregulated in the fibronectin group, while *ITGB4* and *ITGB6* were uniquely upregulated in

cells cultured on the vitronectin surface. This suggests the regulation of integrin expression levels by ECM proteins.

Discussion

Phenotypic differences between the cell lines of a given cancer are common knowledge and have been reported in multiple studies [30, 42, 43], creating the need for a study to choose suitable cancer cell lines for the research question. Our findings suggested that this is also the case for PDAC cell lines, where the cell lines with various backgrounds respond differently to ECM proteins (Figure 1). There are many possible mechanisms behind the differential responses, for example, the primary tumor cell lines (MIA PaCa-2 and PANC1) might express a limited set of integrins that only allow for adhesions to specific ECM proteins, meanwhile, it is also possible that the metastatic cell lines (AsPC-1 and Capan-1) actively secret ECM proteins themselves, enabling them to adhere and spread on surfaces without ECM coatings. Further studies are needed to elucidate the actual mechanisms behind the differential responses to better understand the role of ECM proteins in PDAC progression and metastasis. With this in mind, we chose to use MIA PaCa-2 cells as a model to study the impact of ECM proteins, mainly because of their distinct response to laminin, collagen I, fibronectin, and vitronectin (Figure 1Ai).

MIA PaCa-2 cells spread and proliferate faster on the surface coated with fibronectin and vitronectin, but not on laminin and collagen I. Interestingly, this response is also mirrored in the gemcitabine sensitivity assay and the transcriptomic study, where the cells cultured on fibronectin and vitronectin are significantly different to the no ECM group, while the cells cultured on laminin and collagen I behave similarly to the no ECM group (Figure 2C and 3). From the gemcitabine assay, we observed that the spreading MIA PaCa-2 cells on fibronectin and vitronectin are more sensitive to gemcitabine than the no ECM, laminin, and collagen I groups. Gemcitabine is a nucleoside analog that disturbs and inhibits DNA synthesis, considering the drug mode of action, one may speculate that the cells cultured on fibronectin and vitronectin are more susceptible to the drug simply because of their higher proliferation rate, i.e. higher DNA synthesis activities. However, it is also possible that the presence of ECM proteins regulates other biological processes that modulate the cells' response to gemcitabine [44]. From the transcriptomic study, we also observed that the transcriptomic profiles of cells cultured on fibronectin and vitronectin were distinct from the no ECM, laminin, and collagen I groups. Moreover, MIA PaCa-2 cells express a subset of integrins (Figure S2), which may partially explain their inability to adhere to collagen I, as they express only one possible integrin heterodimer, α10β1, that can recognize collagen I.

However, the inability of MIA PaCa-2 to spread on the laminin surface is somehow intriguing, considering the abundant expression of *ITGA3*, *ITGA6*, and *ITGB4* that potentially can bind to laminin. This discrepancy might be explained by the complex activation and inhibition of integrins by multiple proteins [45, 46] or by the competitive pairings of the alpha and beta subunits that preferentially favor the assembly of a particular set of integrin heterodimers [47]. Interestingly, even though fibronectin and vitronectin are recognized by a similar set of integrins that can bind to the RGD motifs [38, 39], we observed differences in the genes regulated by fibronectin and vitronectin. Several integrins were also differently regulated between the cells cultured on fibronectin and vitronectin (Figure 4B). Follow-up mechanistic studies are required to further elucidate the role of these integrin modulations in response to ECM proteins, for example, one may genetically modulate these integrins and observe the functional response of the cells toward the corresponding ECM proteins.

Considering that cell adhesion and spreading depend on ECM ligand density [48, 49], it is important to note that the observations in this study are limited to the range of ECM concentrations that were used to coat the culture surface, and different responses might be observed when other ECM concentrations are used. It is also important to note that our study is limited to 2D culture, and the cellular responses toward ECM proteins might be different for cells cultured in a 3D scaffold. Indeed, unlike the 2D counterpart, we did not observe growth differences in MIA PaCa-2 spheroids cultured within the 3D polyethylene glycol (PEG) hydrogels containing different ECM proteins (**Figure S4A-B)**. We confirmed the incorporation **(Figure S4C)** and the functionality **(Figure S4D-E)** of the ECM proteins within the PEG hydrogels. Hence, future comparison studies on ECM response within 2D and 3D culture systems are required to fully elucidate the role of ECM proteins on PDAC cellular phenotypes.

Experimental procedures

Cell culture

MIA PaCa-2 and PANC-1, the primary tumor-derived PDAC cell lines, were cultured in DMEM high-glucose media (Genesee Scientific). AsPC-1 and Capan-1, the metastatic lesion-derived PDAC cell lines, were cultured in RPMI 1640 media (Genesee Scientific). Both media were supplemented with 10% fetal bovine serum (FBS) (Sigma-Aldrich) and 1% penicillin and streptomycin (Corning). For experiments to study the effects of ECMs, 2% B-27 (ThermoFisher) was used in place of FBS. Both the PDAC and glioblastoma organoids were acquired from ATCC, as part of the Human Cancer Models Initiative with the organoid name HCM-CSHL-0092-C25

(ATCC PDM-39) and HCM-BROD-0103-C71 (ATCC PDM-121), respectively. Maintenance of the organoid culture was performed following the instructions from ATCC.

Cell proliferation assay

Cells were seeded at 3200-6400 cells/cm^2 and cultured for 6-9 days, and their number was measured every 2-3 days using the CellTitre-Glo 3D cell viability assay (Promega), as described by the manufacturer. Briefly, cells were seeded in a white 96-well plate (Greiner Bio-One) coated with different ECM proteins for 2, 4, 6, and 9 days respectively. The CellTitre-Glo reagent is added to the wells (1:1). The plate reader (BioTek Synergy H1MF multi-mode) shakes the plate for 2 minutes with a delay time of 10 minutes after which the luminescence is measured and recorded. The number of cells is extrapolated from the standard curve generated from the luminescence readings.

ECM proteins coating

Fibronectin (10μg/ml, Sigma-Aldrich), collagen I ((0.1mg/ml, Corning), laminin (10μg/ml, Corning), and vitronectin ((2μg/ml, Sigma-Aldrich) were coated on a plate according to the manufacturer's description. In short, plates are incubated with fibronectin and laminin for 1hr at room temperature. The collagen I is coated overnight at 4°C. The plates are incubated with vitronectin at 37°C for 2hrs after which it's transferred to 4°C overnight. After incubation, excess ECM proteins were removed, and the plates were air-dried at room temperature for 1hr.

Immunofluorescence and image processing

Cells/hydrogels were fixed in 4% formaldehyde (EMS) after which they were permeabilized in 0.5% Triton X-100 (MilliporeSigma) for 10 minutes and blocked with 5% bovine serum albumin (VWR) for 30 mins. For nuclei and F-actin staining, cells were incubated in 2 μg/ml DAPI and phalloidin-tetramethylrhodamine B isothiocyanate (Sigma-Aldrich) respectively, for 1 hour. Images were taken with an Olympus IX71 with an sCMOS camera (Prime 95B, Photometrics) and 10x/0.3NA, 20x/0.75NA, or 40x/0.6NA objective. All the image analysis was done with ImageJ [50].

Gemcitabine treatment

Cells were plated in either an ECM-coated or regular white-bottom 96 well plate and cultured for at least 24 hours prior to the gemcitabine treatment (MilliporeSigma). After 72 h of gemcitabine treatment, the cell number was measured by using the luminescence cell viability assay, as

described above. Gemcitabine sensitivity curves and IC50 values were calculated using Prism v.9 (GraphPad).

Transcriptomics sample preparation and analysis

After culturing the cells on different ECMs, RNA was isolated using the RNeasy Plus Micro Kit (QIAGEN). RNA-Seq library was prepared using the NEBNext Ultra II Directional RNA Library Prep Kit for Illumina (NEB) following the manufacturer's instructions. The library was sequenced on the Novaseq 6000 at Florida State University Translational Science Laboratory. This gives ~20 million reads per sample. The quality of the fastq reads from the sequencing was ascertained with FastQC (version 0.11.9) [51] after which they were aligned with the hg19 human reference genome using the STAR (version 2.7.9a) [52]. Library sizes were scaled and normalized with the median of ratios using the DESeq2 (version 1.32.0) [36]. Differential expression was estimated using the result function in DESeq2. Adjusted p-values, using the Benjamini–Hochberg method were computed and used to filter for significant genes. The heatmap showing the differential gene expression was made using the Pheatmap package in R [53]. To do this, significant differentially expressed genes (adjusted p-value < 0.05, abs($\log_2$FC) > 0.58) in all the ECM proteins were combined and clustered by K-mean (center = 4). Hierarchical clustering was used to cluster the column using Pearson's correlation and Ward.D2. Pathway analysis was done using Enrichr [37]. The significant pathways were filtered using FDR < 0.1.

3D PEG hydrogel culture

Functionalized PEG gel precursors (PEG-NDG-Lys, PEG-Gln) were made as described previously [54]. Briefly, the PEG was functionalized by incubating the 10 kDa 8arm PEG vinyl sulfone (JemKem Technology) with Ac-FKGG-GDQGIAGF-ERCG-NH2 (TG-NDG-Lys) or H-NQEQVSPL-ERCGNH2 (TG-Gln) peptides (GenScript) in triethanolamine (0.3 M, pH 8.0) at 37°C for 20 minutes. The resulting PEG-NDG-Lys and PEG-Gln solutions were dialyzed using a 10,000 MWCO Slide-A-Lyzer dialysis cartridge (ThermoFisher) and lyophilized. The resulting lyophilized precursors were dissolved and reconstituted in deionized water to make a 13.33% w/v stock solution. To make a 10ul gel, 1ul of TBS (50 mM, pH 7.6), 1ul of fibronectin (1mg/ml, Sigma-Aldrich), or collagen I (3.6mg/ml, Corning) or laminin (1mg/ml, Corning) or vitronectin (0.5mg/ml, Sigma-Aldrich), and 1000 cells were added to 4ul of 10% PEG-NDG-Lys + PEG-Gln solution and 1μl distilled water. After the addition of 1ul of thrombin-activated FXIII (Corifact, CSL Behring) that

triggers hydrogel formation, the well plate was flipped and incubated at 37°C for 30 minutes to allow for gelation.

Acknowledgment

The authors would like to thank Dr. Terra Bradley for the careful editing of the manuscript. The authors in this study were supported by startup funds from Florida State University, an award from the Florida Department of Health's Bankhead-Coley Cancer Research Program (award number 21B11) and Live Like Bella Pediatric Cancer Research Initiative (award number 23L06), and a collaborative Trans-Network Project linked to the Physical Science-Oncology Project 5U01 CA214282 from the National Cancer Institute of the National Institutes of Health. S. Ramakrishnan would like to acknowledge funding from the NSF FAMU CREST center award # 1735968 for the current work. Corifact is a gift from CSL Behring. Pancreatic cancer and glioblastoma organoid lines are from the Human Cancer Models Initiative, https://ocg.cancer.gov/programs/HCMI.

References

1. Rahib, L., Smith, B.D., Aizenberg, R., Rosenzweig, A.B., Fleshman, J.M. & Matrisian, L.M. Projecting cancer incidence and deaths to 2030: the unexpected burden of thyroid, liver, and pancreas cancers in the United States. *Cancer Res* **74**, 2913-2921 (2014).

2. Siegel, R.L., Miller, K.D. & Jemal, A. Cancer statistics, 2019. *CA Cancer J Clin* **69**, 7-34 (2019).

3. Islami, F., Ward, E.M., Sung, H., Cronin, K.A., Tangka, F.K.L., Sherman, R.L., Zhao, J., Anderson, R.N., Henley, S.J., Yabroff, K.R. *et al.* Annual Report to the Nation on the Status of Cancer, Part 1: National Cancer Statistics. *J Natl Cancer Inst* (2021).

4. Hidalgo, M. Pancreatic cancer. *N Engl J Med* **362**, 1605-1617 (2010).

5. Kleeff, J., Korc, M., Apte, M., La Vecchia, C., Johnson, C.D., Biankin, A.V., Neale, R.E., Tempero, M., Tuveson, D.A., Hruban, R.H. *et al.* Pancreatic cancer. *Nat Rev Dis Primers* **2**, 16022 (2016).

6. Neesse, A., Michl, P., Frese, K.K., Feig, C., Cook, N., Jacobetz, M.A., Lolkema, M.P., Buchholz, M., Olive, K.P., Gress, T.M. *et al.* Stromal biology and therapy in pancreatic cancer. *Gut* **60**, 861-868 (2011).

7. Feig, C., Gopinathan, A., Neesse, A., Chan, D.S., Cook, N. & Tuveson, D.A. The pancreas cancer microenvironment. *Clin Cancer Res* **18**, 4266-4276 (2012).

8. Perez, V.M., Kearney, J.F. & Yeh, J.J. The PDAC Extracellular Matrix: A Review of the ECM Protein Composition, Tumor Cell Interaction, and Therapeutic Strategies. *Front Oncol* **11**, 751311 (2021).

9. Bijlsma, M.F. & van Laarhoven, H.W. The conflicting roles of tumor stroma in pancreatic cancer and their contribution to the failure of clinical trials: a systematic review and critical appraisal. *Cancer Metastasis Rev* **34**, 97-114 (2015).

10. Stylianopoulos, T., Martin, J.D., Snuderl, M., Mpekris, F., Jain, S.R. & Jain, R.K. Coevolution of solid stress and interstitial fluid pressure in tumors during progression: implications for vascular collapse. *Cancer Res* **73**, 3833-3841 (2013).

11. Mouw, J.K., Ou, G. & Weaver, V.M. Extracellular matrix assembly: a multiscale deconstruction. *Nat Rev Mol Cell Biol* **15**, 771-785 (2014).

12. Kai, F., Drain, A.P. & Weaver, V.M. The Extracellular Matrix Modulates the Metastatic Journey. *Dev Cell* **49**, 332-346 (2019).

13. Schvartz, I., Seger, D. & Shaltiel, S. Vitronectin. *Int J Biochem Cell Biol* **31**, 539-544 (1999).

14. Bonnans, C., Chou, J. & Werb, Z. Remodelling the extracellular matrix in development and disease. *Nat Rev Mol Cell Biol* **15**, 786-801 (2014).

15. Olivares, O., Mayers, J.R., Gouirand, V., Torrence, M.E., Gicquel, T., Borge, L., Lac, S., Roques, J., Lavaut, M.N., Berthezene, P. *et al.* Collagen-derived proline promotes pancreatic ductal adenocarcinoma cell survival under nutrient limited conditions. *Nat Commun* **8**, 16031 (2017).

16. Chen, Y., Kim, J., Yang, S., Wang, H., Wu, C.J., Sugimoto, H., LeBleu, V.S. & Kalluri, R. Type I collagen deletion in alphaSMA(+) myofibroblasts augments immune suppression and accelerates progression of pancreatic cancer. *Cancer Cell* **39**, 548-565 e546 (2021).

17. Tian, C., Clauser, K.R., Ohlund, D., Rickelt, S., Huang, Y., Gupta, M., Mani, D.R., Carr, S.A., Tuveson, D.A. & Hynes, R.O. Proteomic analyses of ECM during pancreatic ductal adenocarcinoma progression reveal different contributions by tumor and stromal cells. *Proc Natl Acad Sci U S A* **116**, 19609-19618 (2019).

18. Pickup, M.W., Laklai, H., Acerbi, I., Owens, P., Gorska, A.E., Chytil, A., Aakre, M., Weaver, V.M. & Moses, H.L. Stromally derived lysyl oxidase promotes metastasis of transforming growth factor-beta-deficient mouse mammary carcinomas. *Cancer Res* **73**, 5336-5346 (2013).

19. Frisch, S.M., Vuori, K., Ruoslahti, E. & Chan-Hui, P.Y. Control of adhesion-dependent cell survival by focal adhesion kinase. *J Cell Biol* **134**, 793-799 (1996).

20. Sottile, J. & Hocking, D.C. Fibronectin polymerization regulates the composition and stability of extracellular matrix fibrils and cell-matrix adhesions. *Mol Biol Cell* **13**, 3546-3559 (2002).

21. Levental, K.R., Yu, H., Kass, L., Lakins, J.N., Egeblad, M., Erler, J.T., Fong, S.F., Csiszar, K., Giaccia, A., Weninger, W. *et al.* Matrix crosslinking forces tumor progression by enhancing integrin signaling. *Cell* **139**, 891-906 (2009).

22. Zhang, C., Wu, M., Zhang, L., Shang, L.R., Fang, J.H. & Zhuang, S.M. Fibrotic microenvironment promotes the metastatic seeding of tumor cells via activating the fibronectin 1/secreted phosphoprotein 1-integrin signaling. *Oncotarget* **7**, 45702-45714 (2016).

23. Wu, S., Zheng, Q., Xing, X., Dong, Y., Wang, Y., You, Y., Chen, R., Hu, C., Chen, J., Gao, D. *et al.* Matrix stiffness-upregulated LOXL2 promotes fibronectin production, MMP9 and CXCL12 expression and BMDCs recruitment to assist pre-metastatic niche formation. *J Exp Clin Cancer Res* **37**, 99 (2018).

24. Hodkinson, P.S., Mackinnon, A.C. & Sethi, T. Extracellular matrix regulation of drug resistance in small-cell lung cancer. *Int J Radiat Biol* **83**, 733-741 (2007).

25. Miyazaki, K. Laminin-5 (laminin-332): Unique biological activity and role in tumor growth and invasion. *Cancer Sci* **97**, 91-98 (2006).

26. Pyke, C., Salo, S., Ralfkiaer, E., Romer, J., Dano, K. & Tryggvason, K. Laminin-5 is a marker of invading cancer cells in some human carcinomas and is coexpressed with the receptor for urokinase plasminogen activator in budding cancer cells in colon adenocarcinomas. *Cancer Res* **55**, 4132-4139 (1995).

27. Huang, C. & Chen, J. Laminin-332 mediates proliferation, apoptosis, invasion, migration and epithelial-to-mesenchymal transition in pancreatic ductal adenocarcinoma. *Mol Med Rep* **23** (2021).

28. Burgos-Panadero, R., Noguera, I., Canete, A., Navarro, S. & Noguera, R. Vitronectin as a molecular player of the tumor microenvironment in neuroblastoma. *BMC Cancer* **19**, 479 (2019).

29. Hayman, E.G. & Ruoslahti, E. Distribution of fetal bovine serum fibronectin and endogenous rat cell fibronectin in extracellular matrix. *J Cell Biol* **83**, 255-259 (1979).

30. Deer, E.L., Gonzalez-Hernandez, J., Coursen, J.D., Shea, J.E., Ngatia, J., Scaife, C.L., Firpo, M.A. & Mulvihill, S.J. Phenotype and genotype of pancreatic cancer cell lines. *Pancreas* **39**, 425-435 (2010).

31. Yang, J., Xu, J., Zhang, B., Tan, Z., Meng, Q., Hua, J., Liu, J., Wang, W., Shi, S., Yu, X. *et al.* Ferroptosis: At the Crossroad of Gemcitabine Resistance and Tumorigenesis in Pancreatic Cancer. *Int J Mol Sci* **22** (2021).

32. Dent, S., Messersmith, H. & Trudeau, M. Gemcitabine in the management of metastatic breast cancer: a systematic review. *Breast Cancer Res Treat* **108**, 319-331 (2008).

33. Hung, S.W., Mody, H.R. & Govindarajan, R. Overcoming nucleoside analog chemoresistance of pancreatic cancer: a therapeutic challenge. *Cancer Lett* **320**, 138-149 (2012).

34. Amrutkar, M. & Gladhaug, I.P. Pancreatic Cancer Chemoresistance to Gemcitabine. *Cancers (Basel)* **9** (2017).

35. Nielsen, M.F., Mortensen, M.B. & Detlefsen, S. Key players in pancreatic cancer-stroma interaction: Cancer-associated fibroblasts, endothelial and inflammatory cells. *World J Gastroenterol* **22**, 2678-2700 (2016).

36. Love, M.I., Huber, W. & Anders, S. Moderated estimation of fold change and dispersion for RNA-seq data with DESeq2. *Genome Biol* **15**, 550 (2014).

37. Chen, E.Y., Tan, C.M., Kou, Y., Duan, Q., Wang, Z., Meirelles, G.V., Clark, N.R. & Ma'ayan, A. Enrichr: interactive and collaborative HTML5 gene list enrichment analysis tool. *BMC Bioinformatics* **14**, 128 (2013).

38. Hynes, R.O. Integrins: bidirectional, allosteric signaling machines. *Cell* **110**, 673-687 (2002).

39. Humphries, J.D., Byron, A. & Humphries, M.J. Integrin ligands at a glance. *J Cell Sci* **119**, 3901-3903 (2006).

40. Bangasser, B.L., Shamsan, G.A., Chan, C.E., Opoku, K.N., Tuzel, E., Schlichtmann, B.W., Kasim, J.A., Fuller, B.J., McCullough, B.R., Rosenfeld, S.S. *et al.* Shifting the optimal stiffness for cell migration. *Nat Commun* **8**, 15313 (2017).

41. Swaminathan, V. & Waterman, C.M. The molecular clutch model for mechanotransduction evolves. *Nat Cell Biol* **18**, 459-461 (2016).

42. Dai, X., Cheng, H., Bai, Z. & Li, J. Breast Cancer Cell Line Classification and Its Relevance with Breast Tumor Subtyping. *J Cancer* **8**, 3131-3141 (2017).

43. Minami, F., Sasaki, N., Shichi, Y., Gomi, F., Michishita, M., Ohkusu-Tsukada, K., Toyoda, M., Takahashi, K. & Ishiwata, T. Morphofunctional analysis of human pancreatic cancer cell lines in 2- and 3-dimensional cultures. *Sci Rep* **11**, 6775 (2021).

44. Topalovski, M. & Brekken, R.A. Matrix control of pancreatic cancer: New insights into fibronectin signaling. *Cancer Lett* **381**, 252-258 (2016).

45. Sun, Z., Costell, M. & Fassler, R. Integrin activation by talin, kindlin and mechanical forces. *Nat Cell Biol* **21**, 25-31 (2019).

46. Harburger, D.S. & Calderwood, D.A. Integrin signalling at a glance. *J Cell Sci* **122**, 159-163 (2009).

47. Anderson, L.R., Owens, T.W. & Naylor, M.J. Structural and mechanical functions of integrins. *Biophys Rev* **6**, 203-213 (2014).

48. Dubin-Thaler, B.J., Giannone, G., Dobereiner, H.G. & Sheetz, M.P. Nanometer analysis of cell spreading on matrix-coated surfaces reveals two distinct cell states and STEPs. *Biophys J* **86**, 1794-1806 (2004).

49. Reinhart-King, C.A., Dembo, M. & Hammer, D.A. The dynamics and mechanics of endothelial cell spreading. *Biophys J* **89**, 676-689 (2005).

50. Schneider, C.A., Rasband, W.S. & Eliceiri, K.W. NIH Image to ImageJ: 25 years of image analysis. *Nat Methods* **9**, 671-675 (2012).

51. S, A. FastQC: A Quality Control Tool for High Throughput Sequence Data [Online]. (2010).

52. Dobin, A., Davis, C.A., Schlesinger, F., Drenkow, J., Zaleski, C., Jha, S., Batut, P., Chaisson, M. & Gingeras, T.R. STAR: ultrafast universal RNA-seq aligner. *Bioinformatics* **29**, 15-21 (2013).

53. Kolde, R. pheatmap: Pretty Heatmaps. R package version 1.0.12. (2019).

54. Gjorevski, N., Sachs, N., Manfrin, A., Giger, S., Bragina, M.E., Ordonez-Moran, P., Clevers, H. & Lutolf, M.P. Designer matrices for intestinal stem cell and organoid culture. *Nature* **539**, 560-564 (2016).

Figure 1

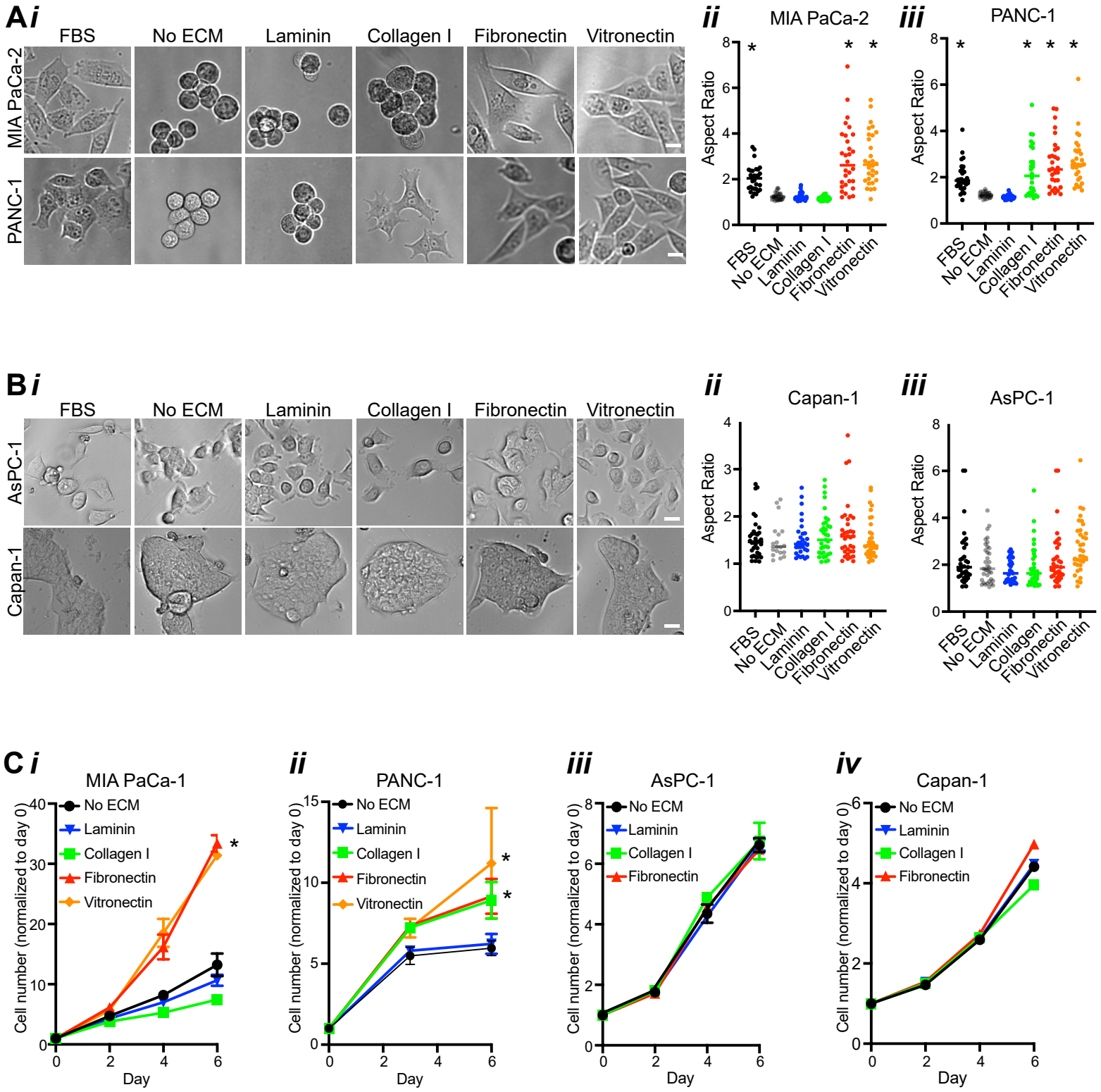
A i
FBS
No ECM
Laminin
Collagen I
Fibronectin
Vitronectin
MIA PaCa-2
PANC-1
ii
MIA PaCa-2
iii
PANC-1
Aspect Ratio
B i
AsPC-1
Capan-1
ii
Capan-1
iii
AsPC-1
C i
MIA PaCa-1
ii
PANC-1
iii
AsPC-1
iv
Capan-1
No ECM
Laminin
Collagen I
Fibronectin
Vitronectin
Cell number (normalized to day 0)
Day

Figure 1. Extracellular matrix proteins have different effects on pancreatic ductal adenocarcinoma (PDAC) cell lines morphology and proliferation.

(A) MIA PaCa-2 and PANC-1 cell lines were cultured in media supplemented with either FBS (FBS) or the serum-free supplement, 2% B27. To investigate the effect of ECM proteins, the cells cultured in 2% B27 were seeded on surfaces without (no ECM) or with ECM protein coating: collagen I, laminin, fibronectin, and vitronectin. Representative images show that MIA PaCa-2 cells (top) adhere and spread in FBS, and on surfaces coated with fibronectin or vitronectin. While they have rounded morphology on no ECM, collagen I, and laminin surfaces. The cellular aspect ratio (AR) is significantly higher in MIA PaCa-2 cells cultured on fibronectin and vitronectin. PANC-1 cells (bottom) also spread in FBS and on surfaces coated with collagen I, fibronectin, and vitronectin. While they remain rounded in no ECM and laminin-coated surfaces. The AR for PANC-1 is significantly higher on surfaces coated with collagen I, fibronectin, and vitronectin (N = 3 experiments, n = 30 cells per group, $*p < 0.01$ vs. no ECM, scale bar: 15 μm)

(B) Representative images show that AsPC-1 (top) and Capan-1 (bottom) morphology do not change regardless of the ECM proteins on which they are cultured. The cellular aspect ratio of Capan-1 and AsPC-1 is not significantly different in ECM proteins compared to no ECM. (N = 3 experiments, n = 30 cells per group, $*p < 0.01$ vs no ECM, scale bar: 15 μm).

(**C**) MIA PaCa-2, PANC-1, AsPC1, and Capan-1 cell lines were cultured on surfaces coated with collagen I, fibronectin, laminin, and vitronectin. The number of cells under each condition was quantified on days 2, 4, and 6 using a luminescent cell viability assay. The number of cells on days 2, 4, and 6 was normalized to the number of cells seeded. MIA PaCa-2 has a higher proliferation rate on fibronectin and vitronectin substrates compared to collagen I, laminin, or well with no ECM coating (i). PANC-1 cultured on collagen I, fibronectin, and vitronectin show a higher proliferation rate compared to those grown on laminin and no ECM (ii). AsPC1 and Capan-1 cultured on different ECM proteins do not show significant differences from those cultured on no ECM plates (iii-iv). (N = 3 experiments, mean±SEM, $*p < 0.01$ vs no ECM).

Figure 2

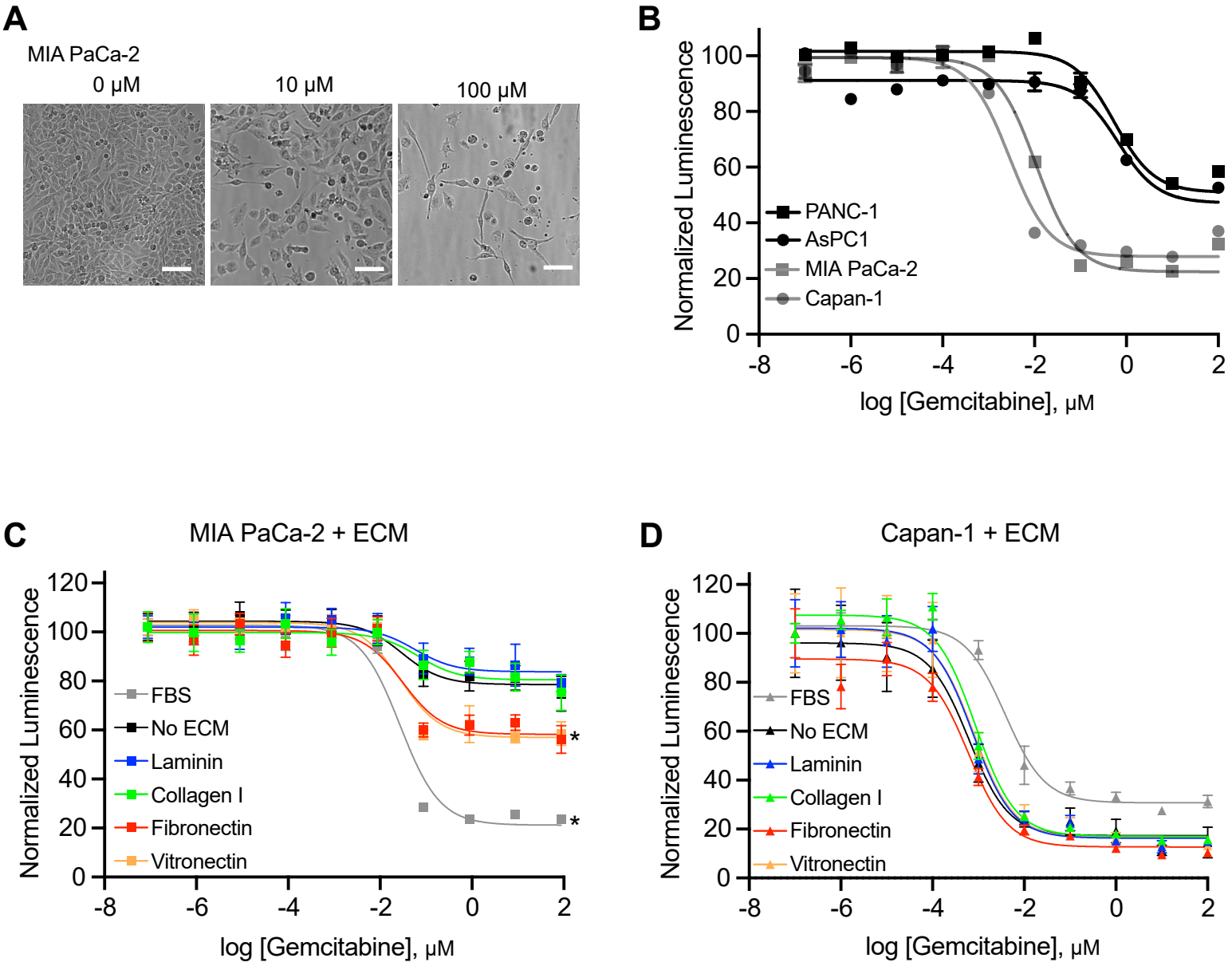
A
MIA PaCa-2
0 μM
10 μM
100 μM
B
Normalized Luminescence
PANC-1
AsPC1
MIA PaCa-2
Capan-1
log [Gemcitabine], μM
C
MIA PaCa-2 + ECM
Normalized Luminescence
FBS
No ECM
Laminin
Collagen I
Fibronectin
Vitronectin
*
*
log [Gemcitabine], μM
D
Capan-1 + ECM
Normalized Luminescence
FBS
No ECM
Laminin
Collagen I
Fibronectin
Vitronectin
log [Gemcitabine], μM

Figure 2. Extracellular matrix proteins alter MIA PaCa-2 sensitivity to gemcitabine.

(A) Cytotoxic effect of gemcitabine on MIA PaCa-2 proliferation was assessed by treating the cells with different concentrations of the drug. Representative images show that the number of surviving cells decreases with increasing concentrations of gemcitabine (scale bar: 100 μm).

(B) AsPC-1, Capan-1, MIA PaCa-2, and PANC-1 were treated with gemcitabine for 72 hrs and the cell numbers were measured using luminescence cell viability assay. MIA PaCa-2 and Capan-1 are more sensitive to the drug treatment, with IC50 of 10.8 and 2.8 nM, respectively, compared to PANC-1 and AsPC-1 with IC50 of 544.2 and 652.9 nM, respectively (N =. 3 experiments, n = 2-3 wells).

(C) MIA PaCa-2 was cultured on surfaces coated with different ECM proteins and then treated with gemcitabine to study how the ECM proteins affect drug response. The cell viability plot shows that the total number of surviving cells after gemcitabine treatment is the lowest for cells cultured in FBS, followed by the cells cultured on fibronectin and vitronectin, and the cells cultured on collagen I and laminin. (*$p < 0.01$ vs no ECM) (N =. 3 experiments, n = 2-3 wells).

(D) Capan-1 response to gemcitabine in the presence of ECM proteins was estimated by culturing the cells on different ECM proteins and quantifying the number of surviving cells after drug treatment. The viability plot shows that ECM proteins do not significantly alter the decrease in the number of surviving cells following drug treatment (N =. 3 experiments, n = 2-3 wells).

Figure 3

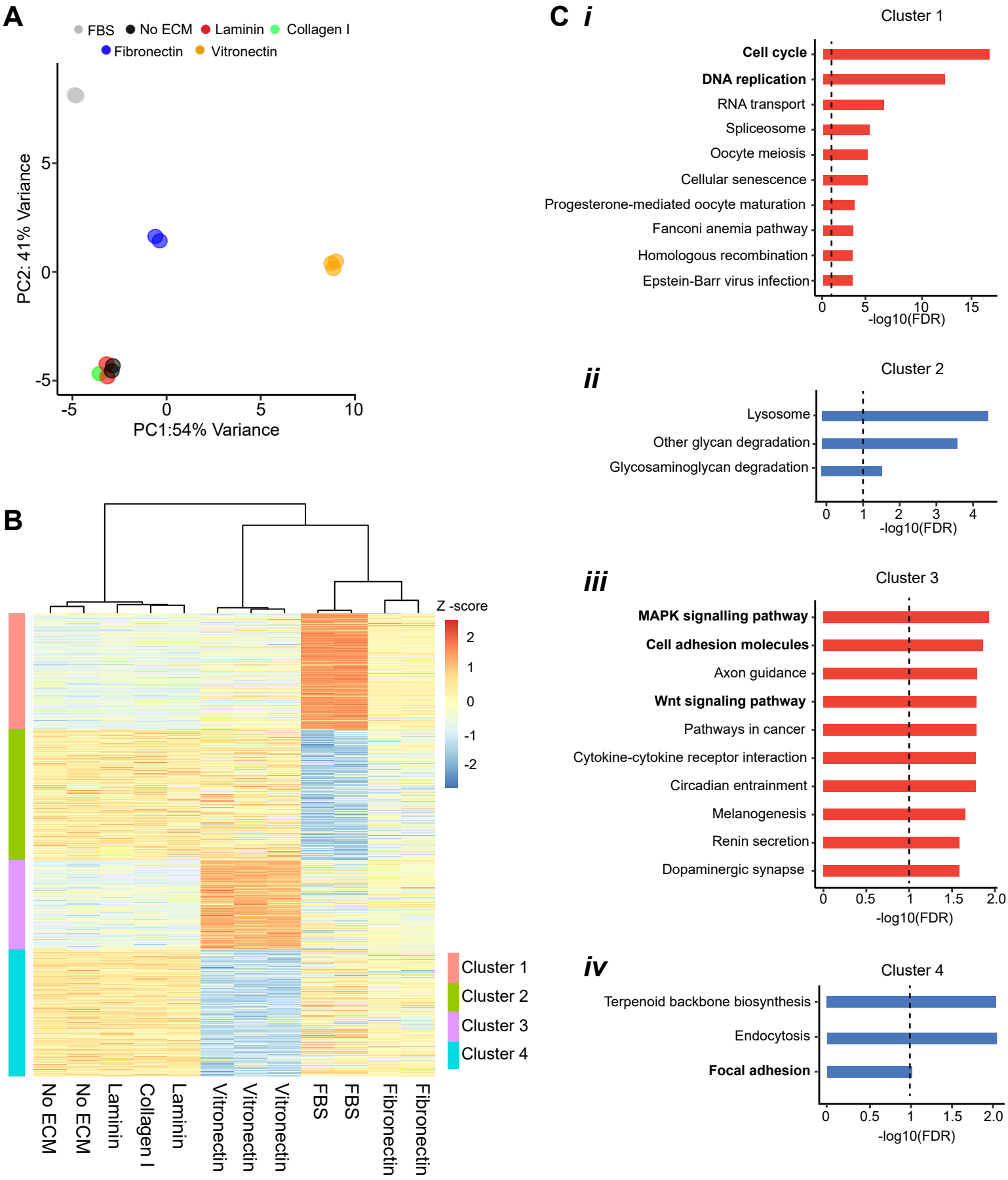
A
FBS
No ECM
Laminin
Collagen I
Fibronectin
Vitronectin
PC2: 41% Variance
PC1:54% Variance
B
Z -score
Cluster 1
Cluster 2
Cluster 3
Cluster 4
No ECM
No ECM
Laminin
Collagen I
Laminin
Vitronectin
Vitronectin
Vitronectin
FBS
FBS
Fibronectin
Fibronectin
C i
Cluster 1
Cell cycle
DNA replication
RNA transport
Spliceosome
Oocyte meiosis
Cellular senescence
Progesterone-mediated oocyte maturation
Fanconi anemia pathway
Homologous recombination
Epstein-Barr virus infection
-log10(FDR)
ii
Cluster 2
Lysosome
Other glycan degradation
Glycosaminoglycan degradation
-log10(FDR)
iii
Cluster 3
MAPK signalling pathway
Cell adhesion molecules
Axon guidance
Wnt signaling pathway
Pathways in cancer
Cytokine-cytokine receptor interaction
Circadian entrainment
Melanogenesis
Renin secretion
Dopaminergic synapse
-log10(FDR)
iv
Cluster 4
Terpenoid backbone biosynthesis
Endocytosis
Focal adhesion
-log10(FDR)

Figure 3. Transcriptomics analysis showing differential gene expression of MIA PaCa-2 cells cultured on surfaces coated with ECM proteins.

(A) MIA PaCa-2 were cultured on different ECM proteins, and they were subjected to RNA-seq. The gene count across the conditions was normalized using the variance stabilizing transformation from DESeq2. The sample clustering was visualized by plotting the first two components resulting from PCA analysis on the x and y axes respectively. PCA analysis showed that cells on ECM proteins (collagen I, laminin) that result in rounded morphology clustered together with cells grown on no ECM. Interestingly, cells cultured on ECM proteins that result in spread morphology (fibronectin and vitronectin) cluster separately from each other, and the cells cultured in FBS.

(B) Heatmap showing normalized read counts of the differentially regulated genes, which were derived from the comparison between MIA PaCa-2 cells cultured on the different ECM proteins against the cells cultured on the surface without ECM coating (no ECM). Clustering analysis of the heatmap reveals that cells cultured on collagen I, laminin, and no ECM protein have a similar expression pattern while those cultured on fibronectin, vitronectin, and FBS show differential gene expression patterns. Cluster 1 comprises genes that are highly upregulated in cells cultured in FBS, while also generally upregulated in cells cultured on vitronectin and fibronectin. Cluster 2 comprises genes that are downregulated in cells cultured in FBS. Clusters 3 and 4 comprise genes that are upregulated and downregulated in cells cultured on a surface coated with vitronectin, respectively. Significant differently expressed genes (adjusted p-value < 0.05, $abs(\log_2 FC) > 0.58$) in all the ECM proteins were combined and clustered by K-mean (with centers = 4) resulting in the color-coded clusters. Hierarchical clustering was used to cluster the column using Pearson's correlation and Ward.D2.

(C) Bar plot showing the KEGG pathways that are enriched by the regulated genes within the clusters derived from the heatmap in Fig. 3B. The genes within each cluster were subjected to pathway analysis using the Enrichr and the top 10 significant pathways were selected (FDR < 0.1). The Red and blue bars indicate upregulated and downregulated pathways, respectively. The dashed line on the bar plot indicates the FDR cut-off.

Figure 4

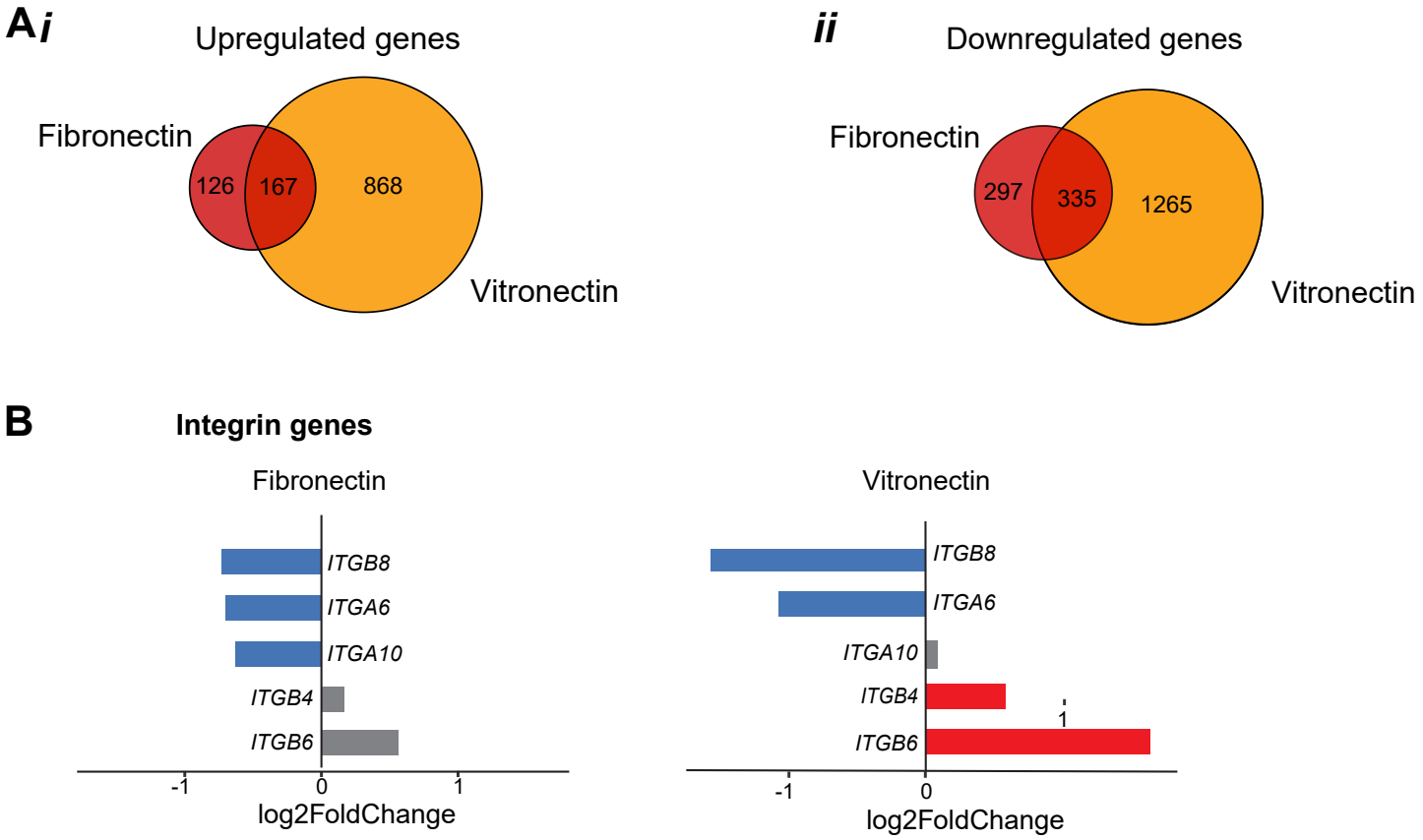
Ai
Upregulated genes
Fibronectin
126
167
868
Vitronectin
ii
Downregulated genes
Fibronectin
297
335
1265
Vitronectin
B
Integrin genes
Fibronectin
ITGB8
ITGA6
ITGA10
ITGB4
ITGB6
-1
0
1
log2FoldChange
Vitronectin
ITGB8
ITGA6
ITGA10
ITGB4
ITGB6
1
-1
0
log2FoldChange

Figure 4. MIA PaCa-2 cells respond differently to fibronectin and vitronectin at the gene expression level

(A) Venn Diagram showing the number of differentially expressed genes (vs. no ECM) that are regulated in both fibronectin and vitronectin (overlap), and also the ones that are unique to fibronectin or vitronectin. The left panel shows that 167 genes are upregulated in cells cultured on fibronectin and vitronectin while 868 and 126 genes are uniquely upregulated in vitronectin and fibronectin, respectively. The right panel shows that 335 genes are downregulated in cells grown on fibronectin and vitronectin, while 1265 and 297 genes are downregulated uniquely in vitronectin and fibronectin, respectively.

(B) Bar plot showing the fold change of integrins in MIA PaCa-2 cell line cultured in fibronectin and vitronectin. Red, blue, and grey bars indicate upregulated, downregulated, and non-significant genes respectively.

Figure S1

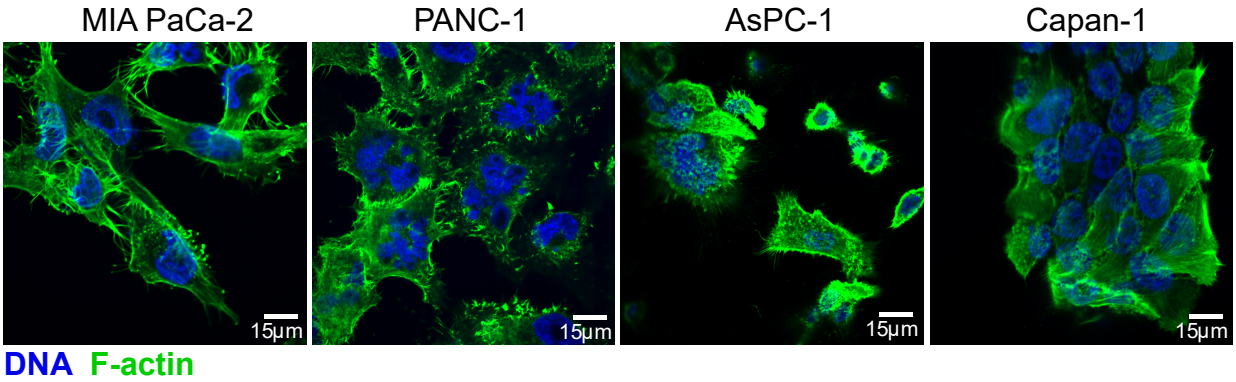

Figure S1: Microscopy images show the morphology of PDAC cell lines.

Image of MIA PaCa-2, PANC-1, AsPC-1, and Capan-1 stained with DAPI (blue) and Phalloidin (green).

Figure S2

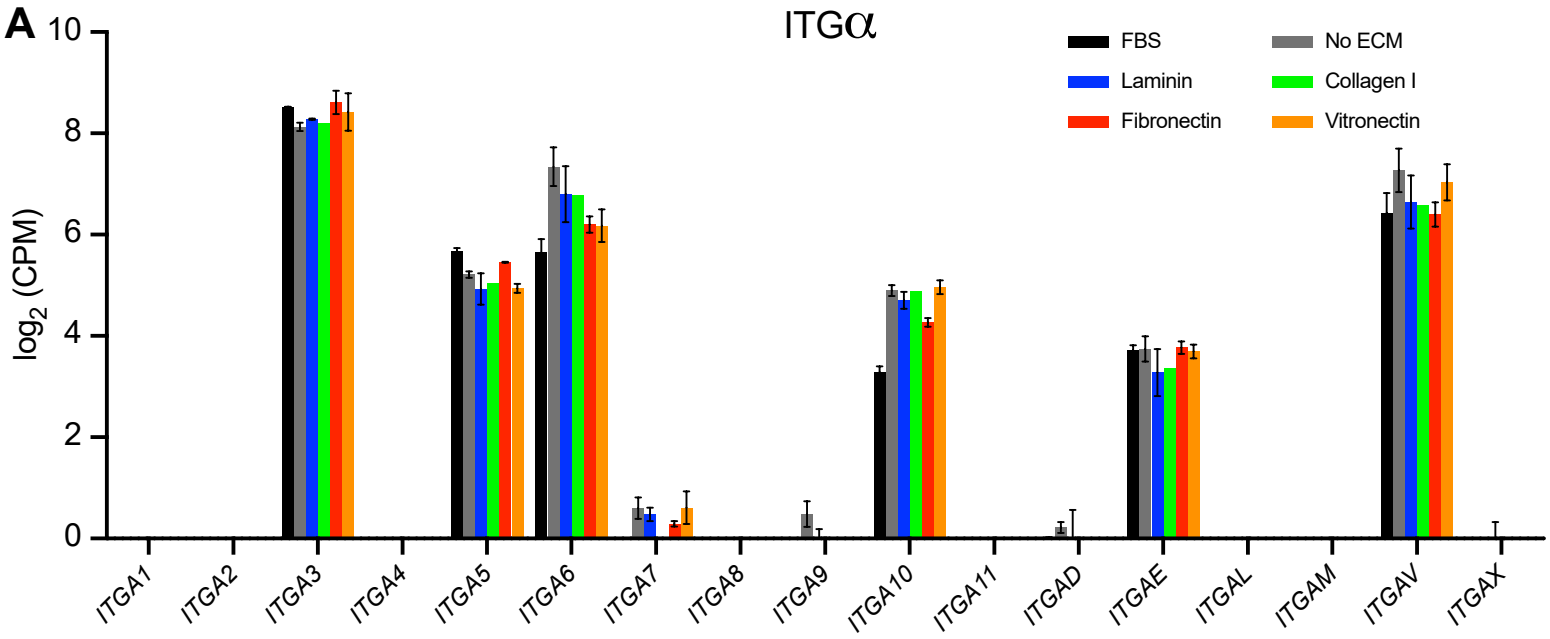
A
ITGα
FBS
No ECM
Laminin
Collagen I
Fibronectin
Vitronectin
log2 (CPM)
0
2
4
6
8
10
ITGA1
ITGA2
ITGA3
ITGA4
ITGA5
ITGA6
ITGA7
ITGA8
ITGA9
ITGA10
ITGA11
ITGAD
ITGAE
ITGAL
ITGAM
ITGAV
ITGAX

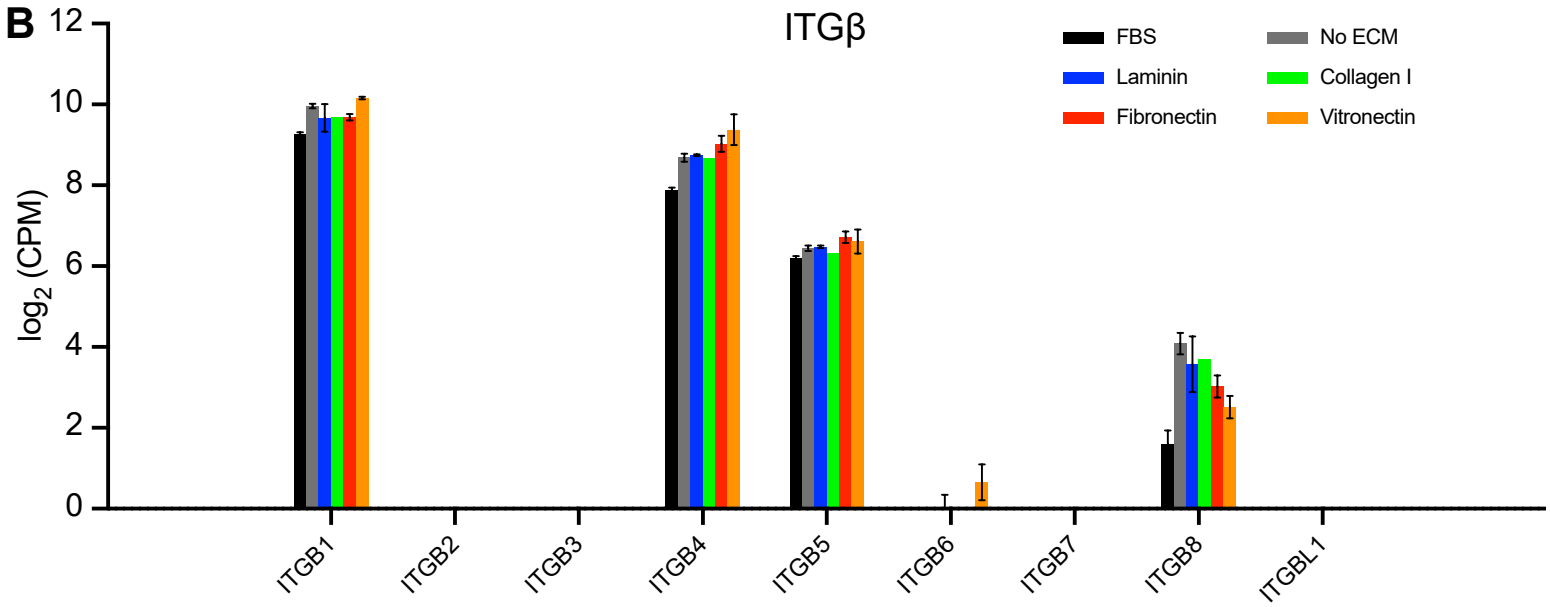
B
ITGβ
FBS
No ECM
Laminin
Collagen I
Fibronectin
Vitronectin
log2 (CPM)
0
2
4
6
8
10
12
ITGB1
ITGB2
ITGB3
ITGB4
ITGB5
ITGB6
ITGB7
ITGB8
ITGBL1

Figure S2: Integrin gene expressions on different ECM proteins.

(A – B) Bar plots showing the normalized read counts of ITGα and ITGβ in MIA PaCa-2 cells cultured on different ECM proteins.

Figure S3

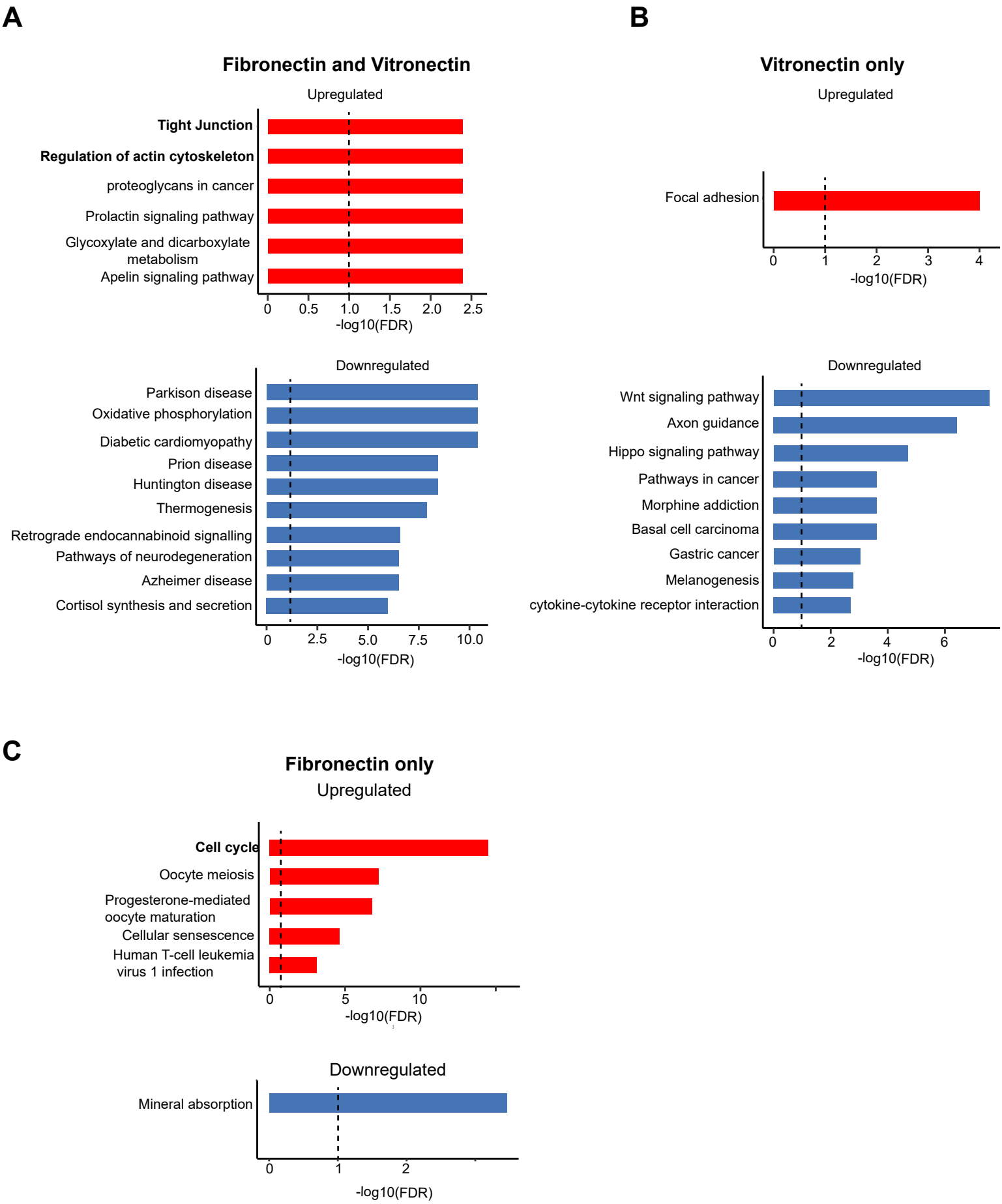
A
Fibronectin and Vitronectin
Upregulated
Tight Junction
Regulation of actin cytoskeleton
proteoglycans in cancer
Prolactin signaling pathway
Glycoxylate and dicarboxylate metabolism
Apelin signaling pathway
0
0.5
1.0
1.5
2.0
2.5
-log10(FDR)
Downregulated
Parkison disease
Oxidative phosphorylation
Diabetic cardiomyopathy
Prion disease
Huntington disease
Thermogenesis
Retrograde endocannabinoid signalling
Pathways of neurodegeneration
Azheimer disease
Cortisol synthesis and secretion
0
2.5
5.0
7.5
10.0
-log10(FDR)
B
Vitronectin only
Upregulated
Focal adhesion
0
1
2
3
4
-log10(FDR)
Downregulated
Wnt signaling pathway
Axon guidance
Hippo signaling pathway
Pathways in cancer
Morphine addiction
Basal cell carcinoma
Gastric cancer
Melanogenesis
cytokine-cytokine receptor interaction
0
2
4
6
-log10(FDR)
C
Fibronectin only
Upregulated
Cell cycle
Oocyte meiosis
Progesterone-mediated oocyte maturation
Cellular sensescence
Human T-cell leukemia virus 1 infection
0
5
10
-log10(FDR)
Downregulated
Mineral absorption
0
1
2
-log10(FDR)

Figure S3: Different pathways are enriched when MIA PaCa-2 cells are cultured on different ECM proteins.

(A - C) Bar plots showing the KEGG pathways that are enriched by the genes regulated in both fibronectin and vitronectin, vitronectin, and fibronectin only. The genes in the overlap of the Venn diagrams in Fig. 4A were subjected to pathway analysis using the Enrichr and a maximum of the top 10 significant KEGG pathways were selected (FDR < 0.1). The red and blue bars indicate upregulated and downregulated pathways respectively.

Figure S4

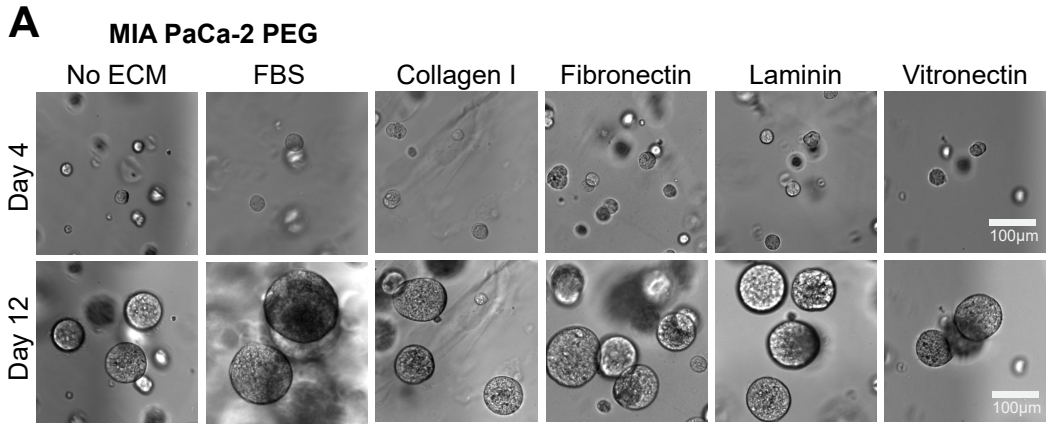
A
MIA PaCa-2 PEG
No ECM
FBS
Collagen I
Fibronectin
Laminin
Vitronectin
Day 4
Day 12
100µm

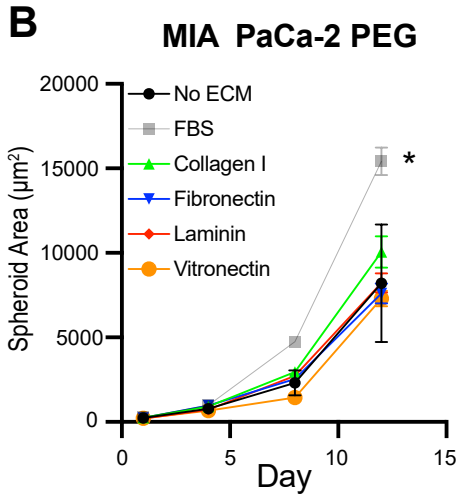
B
MIA PaCa-2 PEG
No ECM
FBS
Collagen I
Fibronectin
Laminin
Vitronectin
Spheroid Area (µm²)
20000
15000
10000
5000
0
0
5
10
15
Day
*

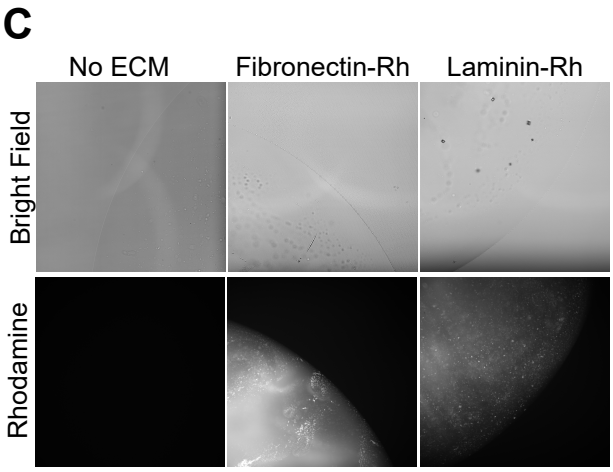
C
No ECM
Fibronectin-Rh
Laminin-Rh
Bright Field
Rhodamine

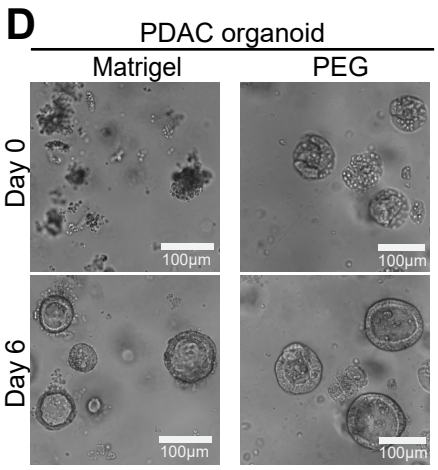
D
PDAC organoid
Matrigel
PEG
Day 0
Day 6
100µm

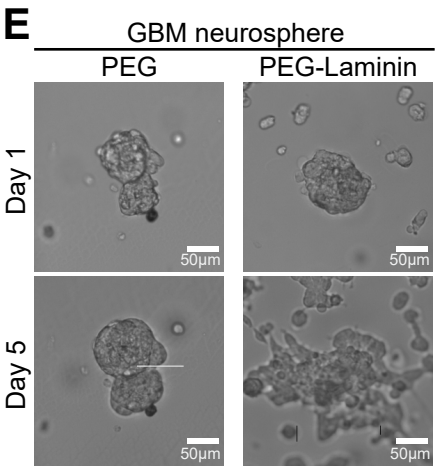
E
GBM neurosphere
PEG
PEG-Laminin
Day 1
Day 5
50µm

Figure S4: MIA PaCa-2 cells grow at a similar rate within PEG hydrogel containing various ECM proteins.

(A) Representative images showing the growth of MIA PaCa-2 spheroids within PEG gels conjugated with different ECM proteins (scale bar: 100 μm).

(B) MIA PaCa-2 cells embedded in PEG gels conjugated with ECM proteins were cultured for 12 days and the growth was quantified by measuring the cross-section area of the spheroids. The plot shows that the MIA PaCa-2 spheroids grow faster when cultured in FBS, however, the spheroids cultured within the PEG gels with various ECM proteins grow at a similar rate as the spheroids embedded in the PEG gels without any ECM proteins (no ECM) (*$p < 0.05$ vs no ECM).

(C) Immunofluorescence shows the incorporation of rhodamine-tagged ECM proteins into the PEG hydrogel.

(D) Patient-derived PDAC organoid, PDM39, was cultured in Matrigel and PEG for 6 days. Representative images show that the organoid grows both in PEG and Matrigel.

E) Patient-derived glioblastoma organoid, PDM121, was cultured in PEG with no ECM (PEG) and PEG with laminin (PEG-Laminin). Representative images show PDM121 invasion only in PEG-Laminin.